

Positively Charged Surfaces Increase the Flexibility of DNA

Alessandro Podestà,* Marco Indrieri,* Dorian Brogioli,[†] Gerald S. Manning,[‡] Paolo Milani,* Rosalinda Guerra,[†] Laura Finzi,[†] and David Dunlap[§]

*Department of Physics, INFN and CIMAINA, and [†]Department of Biology and CIMAINA, University of Milan, Milan, Italy;

[‡]Department of Chemistry and Chemical Biology, Rutgers University, Piscataway, New Jersey; and [§]ALEMBIC, San Raffaele Scientific Institute, Milan, Italy

ABSTRACT Many proteins “bind” DNA through positively charged amino acids on their surfaces. However, to overcome significant energetic and topological obstacles, proteins that bend or package DNA might also modulate the stiffness that is generated by repulsions between phosphates within DNA. Much previous work describes how ions change the flexibility of DNA in solution, but when considering macromolecules such as chromatin in which the DNA contacts the nucleosome core each turn of the double helix, it may be more appropriate to assess the flexibility of DNA on charged surfaces. Mica coated with positively charged molecules is a convenient substrate upon which the flexibility of DNA may be directly measured with a scanning force microscope. In the experiments described below, the flexibility of DNA increased as much as fivefold depending on the concentration and type of polyamine used to coat mica. Using theory that relates charge neutralization to flexibility, we predict that phosphate repulsions were attenuated by ~50% in the most flexible DNA observed. This simple method is an important tool for investigating the physiochemical causes and molecular biological effects of DNA flexibility, which affects DNA biochemistry ranging from chromatin stability to viral encapsulation.

INTRODUCTION

DNA is an exceptionally stiff polymer which ought to present significant energetic and topological obstacles to proteins that bend or package DNA. For example, although histones bristle with positive charges that contact the DNA, the overall affinity may reflect more than simple electrostatic coupling (1). In fact reconstitution experiments with systematic base substitutions have shown that nucleosome stability correlates with increasingly flexible DNA (2). The flexibility of an elastic polymer such as DNA is usually quantified by the persistence length, which is ~53 nm in physiological solution. This is at least an order of magnitude greater (stiffer) than that of common synthetic chains. Such stiffness appears to have an electrostatic component, since asymmetric neutralization of phosphates in oligonucleotides induces bending (3,4). If a significant part of DNA's rigidity is due to charge repulsions between phosphates along the double helix, it could be modulated electrostatically (5,6). Decades ago, Frontali and colleagues directly measured persistence length from electron micrographs of DNA spread using cytochrome C and demonstrated that the concentration of surrounding ions inversely affected the persistence length (7). Subsequently, a number of groups have confirmed this behavior using electron microscopy, scanning force microscopy, or single molecule manipulation to measure the flexibility of DNA. In some cases supercoiling (8,9) was used as an index of flexibility, whereas others used indirect (10–12) or direct (13) methods to determine the persistence length.

Increased flexibility due to attenuated repulsions should also facilitate packaging of DNA for mitosis and encapsulation, and indeed Evilevitch et al. have shown that spermine reduces the pressure due to tightly packed DNA inside phage capsids (14). They attributed the pressure mainly to electrostatic repulsions between negatively charged double helices, but the diameters of some capsids are of the same magnitude as the persistence length of DNA and several reports show that polyamines reduce the persistence length of DNA to ~40 nm (8,10,15). To study charge-induced, electrostatic softening of the DNA, we have taken a cue from cells, which produce several polyamines that are essential for cell growth (16,17). These polyvalent cations have high affinity for DNA and can attenuate repulsions between negative charges on the phosphates (18) such that DNA molecules aggregate in dilute solutions (19–21). In this report we describe as much as fivefold increases of DNA flexibility measured in scanning force micrographs depending on the type and density of natural or artificial polyamines (22) used to prepare the DNA substrate. Our data highlight the electrostatic tension that stiffens DNA and how increasing densities of polyamines may reduce charge repulsions as much as 50% and dramatically increase the flexibility of this extraordinary polymer.

MATERIALS AND METHODS

DNA preparation

The 300 bp fragment was amplified from plasmid pBend2 using PCR with the following primers: (forward) 5'-TAT CAC GAG CCC TTT CGT CTT CAA-3' and (reverse) 5'-ACC GCA TTA AAG CTT GGA TCC CTC-3'. The PCR product was electrophoretically isolated and purified using a kit (Qiagen, Venlo, Netherlands). Repeated agarose digestions were often

Submitted April 15, 2005, and accepted for publication June 24, 2005.

Address reprint requests to David Dunlap, ALEMBIC, DIBIT 3A3, San Raffaele Scientific Institute, Via Olgettina 58, 20132 Milan, Italy. Tel.: 39-022-643-4636; Fax: 39-022-643-4813; E-mail: dunlap.david@hsr.it.

© 2005 by the Biophysical Society

0006-3495/05/10/2558/06 \$2.00

doi: 10.1529/biophysj.105.064667

necessary to completely eliminate the agarose. For deposition the DNA was diluted to ~ 1 nM in 20 mM HEPES pH 7.9, 60 mM KCl, and 1 mM DTT.

For longer fragments plasmid pS3 was cut with restriction enzymes SalI and SphI to produce a 449 base pair fragment or used as a template for PCR with the following primers: (forward) 5'-AAC CAT GAC ATC AGC GGG ACT TCC-3' and (reverse) 5'-AGG GTG GAC CCC GAC TTA ATC ACG -3' to produce a 707 bp fragment. The 707 bp fragment was isolated by gel electrophoresis, purified using a kit (Qiagen) and resuspended in 1.0 M tris(hydroxymethyl)methylamine-HCl, pH \sim 8, with 0.1 M ethylenediaminetetraacetic acid (TE), whereas the 449 bp fragment was isolated by gel electrophoresis, purified by phenol-ether extraction, and resuspended in TE. The 896 bp DNA fragment was produced by digesting plasmid pUC19 with Pvu 1, isolated by gel electrophoresis, purified using a kit (Qiagen) and resuspended in TE. The DNA was diluted to working concentrations of ~ 1 nM in 20 mM HEPES pH 7.9, 50 mM NaCl, 5 mM MgCl₂, 0.5 mM EDTA, 1 mM DTT.

Specimen preparation and AFM imaging

Poly-L-ornithine (P3655 or P5666, Sigma, St. Louis MO) or spermidine (Sigma) was used at the indicated concentrations to coat mica. Poly-L-ornithine P3655 is a polydisperse preparation with an estimated molecular weight of 30,000–70,000. Instead poly-L-ornithine P5666 has a molecular weight of ~ 1000 . Since these poly-L-ornithines have a wide distribution of molecular weights, the relative concentrations of amine moieties can be best compared using weight/liter or equivalents of amine/liter. 10 μ l of a polyamine solution was spotted on a 9 mm diameter disc of freshly cleaved, ruby muscovite mica (Ted Pella, Redding, CA) and incubated for 1–2 min. When the mica surface cleaved completely by peeling away a layer with adhesive tape, the droplet spread out to cover the entire surface. The sample was washed dropwise with several milliliters of HPLC-grade water (Sigma), and then dried with a gentle stream of nitrogen. The resulting polyamine-coated surface is slightly rougher than bare mica (root mean-square ≤ 0.2 nm (22)) and ~ 1 –3 nm thick. Five μ l of the DNA solution was then spotted on the polyamine-coated mica surface, incubated for 1–5 min, and washed and dried in a similar way. In the case of uncoated mica, 5 μ l of the Mg²⁺-containing DNA solution were directly spotted onto freshly cleaved mica and washed and dried as described above.

Samples were imaged in a dry, nitrogen atmosphere, using Multimode Nanoscope IIIa and IV AFMs (Veeco, Dourdan, France). The AFM was operated in Tapping Mode with single crystal silicon tips (resonance frequency 200–300 kHz), at scan rates of 1.5–3 Hz, over scan areas from 0.5 to 2.0 microns wide (sampling resolution ~ 1 nm/pixel).

Data analysis

AFM images of DNA were DC-filtered in the slow-scan direction, and then each DNA molecule was manually traced to establish the spatial coordinates of its backbone with 2–4 nm resolution. The traces, consisting typically of 200–700 curves, were analyzed using custom MATLAB (MathWorks, Natick, MA) routines. The routines evaluate the following characteristic functions describing the DNA configuration: the mean squared angle $\langle \theta^2 \rangle(\Delta L)$ between points along the DNA backbone separated by ΔL , and the mean squared, end-to-end distance $\langle R^2 \rangle(\Delta L)$ of DNA segments with length ΔL .

The rigidity of the DNA chain is characterized by the extinction length l of the average $\cos(\theta(\Delta L))$:

$$\langle \cos(\theta(\Delta L)) \rangle = e^{\left(\frac{-\Delta L}{l}\right)}. \quad (1)$$

This relation follows from the assumption that the orientation of each segment of the DNA molecule exhibits small, symmetric fluctuations around the direction of its neighbor. We identify this length with twice the persistence length, P , of the molecule in analogy with the two-dimensional wormlike chain (WLC) model in which the angle fluctuations are exactly Gaussian over the whole range of segment lengths.

In the limit of small angles and small separations, Eq. 1 becomes

$$\langle \theta^2 \rangle(\Delta L) = \frac{\Delta L}{P} \quad \text{for } \Delta L \leq 2P, \quad (2)$$

which allows the determination of the values of the persistence length via a linear fit. The persistence length can also be extracted from the $\langle R^2 \rangle(\Delta L)$ curves by fitting with the following expression for the two-dimensional WLC model:

$$\langle R^2 \rangle(\Delta L) = 4P\Delta L \left[1 - \frac{2P}{\Delta L} \left(1 - e^{-\frac{\Delta L}{2P}} \right) \right]. \quad (3)$$

We typically obtained good fits up to $\Delta L \sim 2$ –6 P and some data fit the WLC $\langle R^2 \rangle(\Delta L)$ curve across the whole range of separations, ΔL . The values of P determined using either expression were very similar and the reported values are weighted averages.

RESULTS

Fig. 1 is a representative pair of images of DNA molecules on a mica surface prepared by precoating the mica with solutions of either 100 μ g/ml (upper) or 0.018 μ g/ml (lower) high molecular weight poly-L-ornithine (PO-49). It is evident that the molecules on the surface coated with dilute PO-49 were more extended (Fig. 1, lower). As the poly-L-ornithine concentration was increased, the positive charge density on the surface also increased, and the DNA molecules assumed more compact conformations with dramatically decreased, average end-to-end distance (Fig. 1, upper). However, on all of the surfaces described in this report the DNA molecules had contour lengths commensurate with the B-form (22).

Persistence lengths were measured from tracings of molecules in similar images recorded for DNA deposited on mica coated with different concentrations and types of polyamines (Table 1). As a control, uncoated mica was used and the measured persistence length was 56 nm, in accord with previous reports (10,13). When the mica was coated with 0.18 μ g/ml, 1 kDa poly-L-ornithine (PO-1) or 0.5 μ g/ml spermidine, the persistence length decreased to 42 or 36 nm, respectively. A 10-fold lower concentration of PO-49 (0.018 μ g/ml) was more effective than PO-1 (and spermidine) and decreased the persistence length to 33 nm. Instead an equal amount (0.18 μ g/ml) of PO-49, used to coat the mica, further reduced the persistence length of DNA to 27 nm. Finally, coatings with 100 μ g/ml PO-1 or PO-49 dropped the persistence length of DNA to 16 or 11 nm, respectively, a four- to fivefold reduction of the typical value measured in physiological solution. Others have observed a similar reduction for concentrated PO-49 (23).

On moderately or weakly charged surfaces, DNA molecules behaved as two-dimensional wormlike chains. Fig. 2 shows the mean of the squared, end-to-end distance as a function of segment lengths along the contours of 896 bp DNA molecules deposited on mica coated with PO-1 (0.18 μ g/ml) or spermidine (0.5 μ g/ml). As a reference, there is

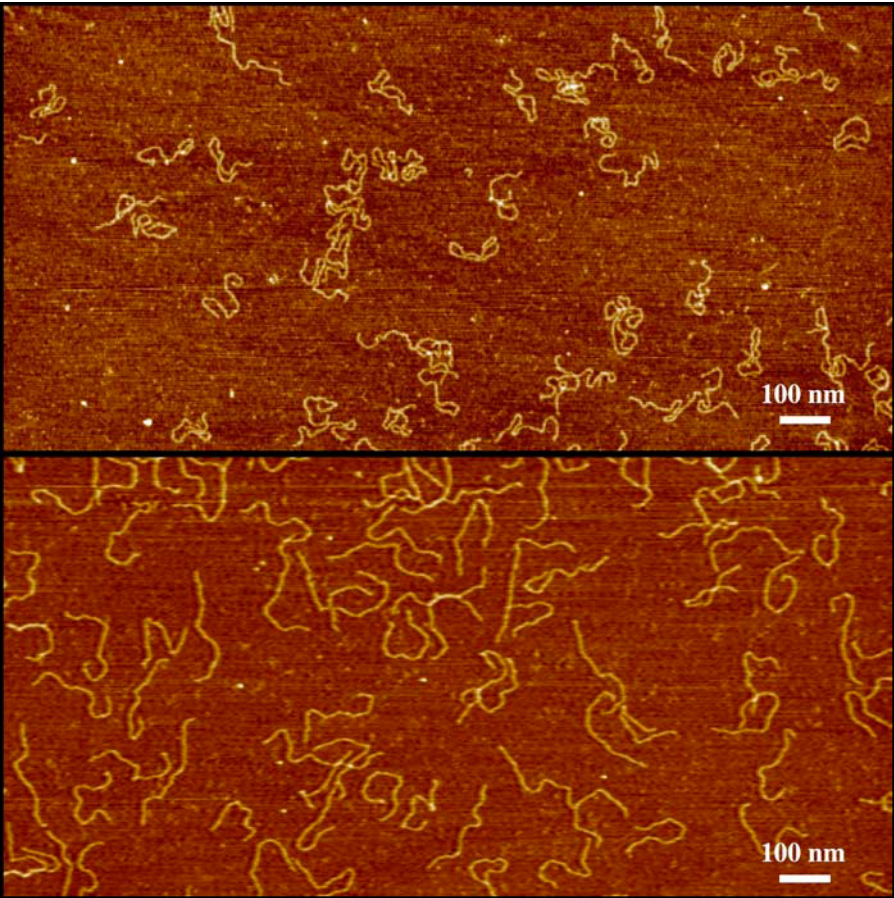


FIGURE 1 DNA molecules (896 bp) are more compact on 100 $\mu\text{g/ml}$, 49 kDa poly-L-ornithine (*upper*) than on 0.018 $\mu\text{g/ml}$, 49 kDa poly-L-ornithine (*lower*).

also a curve for 707 bp DNA molecules deposited on freshly cleaved mica in Mg^{+2} -containing buffer. Rivetti et al. have shown that DNA in solutions containing Mg^{+2} exhibits two-dimensional, wormlike chain conformations on mica (13). Indeed the experimental data superimpose exactly upon a theoretical curve for a two-dimensionally equilibrated WLC with a persistence length of 56 nm. Similarly, the DNA deposited on poly-L-ornithine- and spermidine-coated mica

corresponded to WLC curves with persistence lengths of 42 and 37 nm, respectively, over the entire range of segment lengths along the contours of the molecules. The wormlike chain behavior of this DNA is clear evidence that the molecules deposited on these surfaces is not electrostatically trapped in configurations reminiscent of their three-dimensional forms but readily assume an equilibrium distribution accessible to molecules free to move in two dimensions.

TABLE 1 Measured persistence lengths

P (nm)	Coating			bp	No. molecules
	Type	($\mu\text{g/ml}$)	($\mu\text{Eq/l}$)		
56.5 ± 1	-	-	-	707	633
42.5 ± 1	PO 1	0.18	0.84	896	170
36.4 ± 0.1	spermidine	0.50	5.9	896	444
32.6 ± 0.5	PO 49	0.018	0.084	896	416
26.6 ± 0.2	PO 49	0.18	0.84	896	229
16.1 ± 0.1	PO 1	100	470	896	188
11.8 ± 0.1	PO 49	100	470	449	327
11.4 ± 0.7	PO 49	100	470	300	281
11.3 ± 0.2	PO 49	100	470	707	273
11.3 ± 0.1	PO 49	100	470	896	434

The persistence lengths were measured for DNA fragments deposited on surfaces with different degrees of positive charge density (PO-1, 1 kDa poly-L-ornithine; PO-49, 49 kDa poly-L-ornithine).

Instead, ensembles of DNA deposited on highly charged, poly-L-ornithine-coated mica deviate significantly from wormlike chain behavior for segments longer than 80–100 nm. Fig. 3 shows the $\langle R^2 \rangle / \Delta L$ curves of 300, 449, 707, and 896 bp DNA molecules deposited on PO-49 at 100 $\mu\text{g/ml}$. These fragments resemble wormlike chains over distances $< \sim 100$ nm, but segments of lengths > 100 nm have shorter end-to-end distances than expected from the WLC model. Fitting $\langle R^2 \rangle / \Delta L$ data for segments < 100 nm to WLC functions produced persistence lengths of ~ 11 nm.

The change of the persistence length as a function of the surface charge density is highlighted in Fig. 4, which shows the $\langle R^2 \rangle / \Delta L$ curves measured for 896-bp DNA molecules deposited on mica coated with PO-49 at different concentrations. Overall the persistence lengths inversely scaled with the concentration of PO-49 used to coat the mica, and varying the molecular weight (1 or 49 kDa) and/or concentration

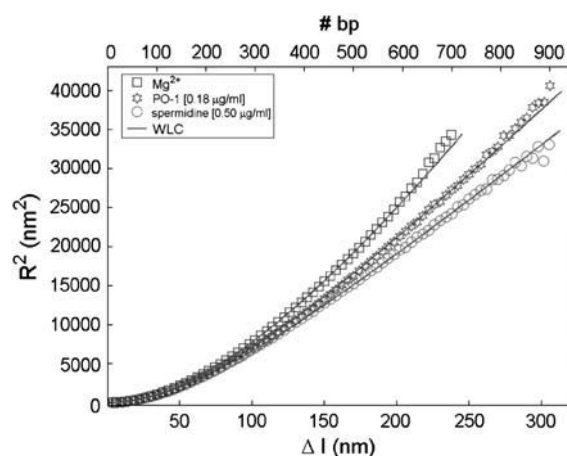


FIGURE 2 DNA deposited on untreated mica, mica coated with 0.18 $\mu\text{g/ml}$ of 1 kDa poly-L-ornithine, or 0.5 $\mu\text{g/ml}$ of spermidine exhibits ensembles of wormlike chain configurations. The average end-to-end distances of all possible segments from the tracings of molecules in each condition were plotted as functions of the average curvilinear (contour) lengths for the same segments. The data were well fitted by curves representing theoretical wormlike chains with persistence lengths of 56, 42, or 37 nm for untreated (Mg^{+2} -mediated deposition), poly-L-ornithine-, or spermidine-coated mica, respectively.

(four orders of magnitude) of poly-L-ornithine changed the persistence length from 56 to 11 nm in steps as small as 4 nm (see Table 1). Thus these parameters can be used to finely tune the resulting persistence length of deposited DNA.

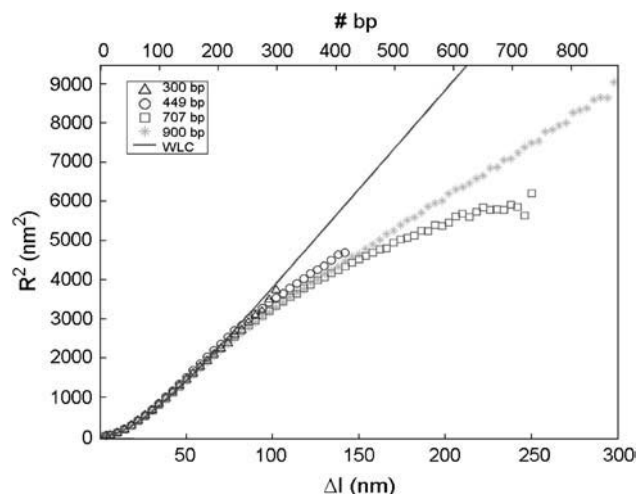


FIGURE 3 DNA deposited on highly charged surface deviates from wormlike chain configurations beyond 80–100 nm of curvilinear distance. DNA fragments of 300, 449, 707, and 896 bp were deposited on mica treated with 100 $\mu\text{g/ml}$ of 49 kDa poly-L-ornithine, imaged, traced, and analyzed as in Fig. 2. The initial portions of these curves superimpose, demonstrating that the differently sized molecules established similar ensembles. Data for the 300-bp fragment were fit to a theoretical wormlike chain with a persistence length of ~ 11 nm throughout its entire contour length of ~ 100 nm. The longer fragments exhibited the same initial behavior, but adopted more compact conformations than expected for wormlike chains longer than 100 nm.

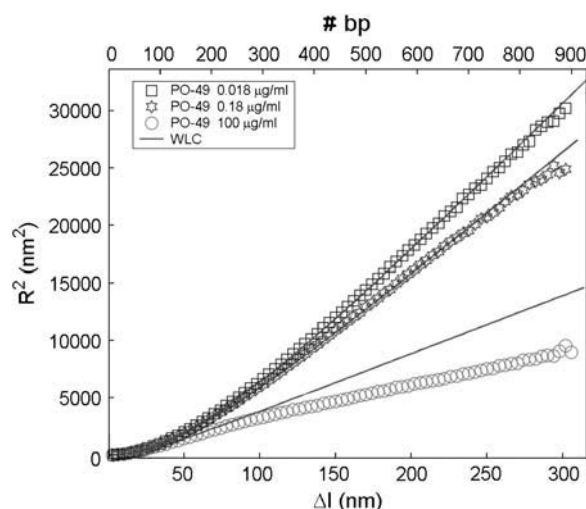


FIGURE 4 Persistence length decreased with increasing surface charge. DNA (896 bp) was deposited on mica coated with 49 kDa poly-L-ornithine, imaged, traced, and analyzed as in Figs. 2 and 3. DNA deposited on mica treated with 0.018, 0.18, or 100 $\mu\text{g/ml}$ of PO-49 had persistence lengths of 32, 27, and 11 nm, respectively.

DISCUSSION

Figs. 3 and 4 clearly demonstrate that the persistence length of DNA on highly charged surfaces cannot be measured by simply relating the average end-to-end distance of an ensemble of molecules to their average contour length using a WLC relationship. One difficulty is the discrimination of two-dimensionally “equilibrated” molecules from those that are “kinetically trapped” (13). In fact, we have measured DNA that, on the most highly charged surfaces, equilibrates locally while remaining compact on larger scales, and for such a specimen the distinction between trapping and equilibrium would depend upon the scale of a simple end-to-end distance measurement. This deviation from WLC behavior occurred at the same segment length for three differently sized DNA fragments and therefore does not appear to be the result of kinetic trapping of DNA on the surface. If DNA molecules had been kinetically limited from achieving an equilibrated ensemble, then smaller molecules would have been expected to more readily reach equilibrium. Instead the 449, 707, and 896 bp DNA molecules all began to deviate from WLC behavior at the same segment length (Fig. 3).

On the other hand, DNA deposited on moderately charged surfaces clearly formed ensembles of wormlike chains indicating free mobility after contact with the surface. Such behavior was expected on the basis of Raman spectra interpreted to derive from nonspecific electrostatic interactions between phosphates and either spermidine or spermine bound to B-form DNA (24). It is noteworthy that a surface prepared with spermidine reduced the persistence length to a lesser extent than those with poly-L-ornithine (Table 1). The persistence length on surfaces prepared with both poly-L-ornithines at 0.84 microequivalents of amine/liter was shorter than that

found for DNA deposited on mica coated with spermidine in a solution of 5.9 microequivalents of amine/liter. It may be that in comparison to the linear spermidine molecules, the branched side chains of poly-L-ornithine molecules more effectively embrace DNA molecules to more effectively attenuate phosphate charge repulsions.

However both naturally occurring and artificial polyamines reduced the repulsive electrostatic interactions among the negatively charged phosphate groups on the DNA backbone that stiffen the double helix. Mirzabekov and Rich first suggested that if the phosphate charge were neutralized on one side of the DNA, the double helix would then bend toward the neutralized side (25). A quantitative estimate on the basis of polyelectrolyte theory indicated that this effect might result in large bend angles (26). In fact, DNA oligonucleotides with phosphates asymmetrically neutralized by methylphosphonate substitution bent significantly toward the side of chemical modification (27) and minimum-energy simulations revealed similar results (4,28). DNA apparently bends, or buckles, into the groove bordered by charge-neutralized phosphate groups, and both experiments and computations suggest that also DNA-bending proteins may operate, at least partially, by asymmetric phosphate neutralization (29–31).

Since phosphate repulsions apparently stiffen DNA, then attenuating such repulsions might render the DNA more flexible. Theory can provide the following relation between the persistence length of a DNA with all of its phosphate groups “charge neutralized”, P , and the persistence length of the same DNA with all phosphates in their fully ionized “−1” valence, P_0 ,

$$P = \frac{2}{\pi R^2} \left[\frac{\beta P_0}{2(\xi - 1) - \ln(\kappa b)} \right]^{\frac{1}{2}}, \quad (4)$$

in which R is the radius of the double helix (5). The quantity β is the Bjerrum length, the distance between two unit charges in pure solvent (no other ions) at which the electrostatic interaction energy is kT . This equals 0.71 nm in water at room temperature. The electrostatic screening effect of salt is taken into account by the linear Debye screening parameter κ . Its reciprocal, the screening length κ^{-1} , is equal to 0.96 nm in 0.1 M univalent salt. The dimensionless quantity $\xi = \beta/b$ in Eq. 4 is a measure of the axial charge density of the DNA (b is the average axial spacing between phosphates, 0.17 nm) and indicates the importance of non-linear electrostatic effects (6). The model upon which Eq. 4 is based represents DNA as an elastic rod that buckles under the electrostatic stress generated by the neutralization of phosphate charge. It is not applicable to highly flexible polymers that do not behave like stiff rods.

The persistence length of repulsion-free (hereafter referred to as “null”) DNA predicted by Eq. 4 is 7.0 nm, which is somewhat smaller than the lowest value, 11 nm, measured for DNA deposited on a poly-L-ornithine surface. Possible reasons may be the approximations inherent in the theoretical model and analysis. Another reason may be that

“null” DNA is 100% charge-neutralized DNA, whereas the poly-L-ornithine surfaces used in these measurements might not completely eliminate repulsions between all phosphates of the adsorbed DNA.

The theory may be extended to the case of DNA with a fraction of effectively neutralized phosphate charges (x) intermediate between zero (fully ionized DNA) and unity (“null” DNA). Table 2 lists calculated persistence length values P for various values of x . The lowest persistence length that was measured is calculated to occur when the phosphates are ~60% neutralized. Perhaps the most highly charged poly-L-ornithine coated surface attenuated about half of the repulsions between DNA phosphates. This estimation is significant, since reports in the literature indicate that DNA condensation requires 90% neutralization of the phosphate charge (18). Below this level DNA should not condense (lateral contact between segments) and indeed the compact DNA such as is shown in Fig. 1 *a* does not appear to be condensed.

Using a simple procedure we have shown that the persistence length of *B*-form DNA adsorbed onto a polyamine-coated surface can be systematically reduced as much as fivefold below the canonical 50–60 nm found in physiological salt solutions. This method might be applied to precisely control the physiochemistry of DNA. For instance, reducing the inherent stiffness of DNA could permit the fabrication of smaller DNA devices (32) and facilitate the insertion of DNA in nanometer-scaled pores or channels (33). The above measurements can serve as initial guidelines for using polyamines in such endeavors.

These measurements also highlight the dominant electrostatic component of DNA stiffness. Moderate attenuation of charge repulsions in the above conditions did not provoke collapse or kinking of DNA but greatly reduced the persistence length. Such behavior is to be expected given the bulk of the DNA molecule, which resists compression. In fact, the contour length of DNA did not vary, whereas persistence length decreased as much as fivefold.

Several reports in the literature support the idea that electrostatically induced softening of DNA is likely to be important in a variety of biological phenomena including DNA packaging in phage capsids (14), the determination of

TABLE 2 Persistence length versus fractional charge neutralization

x	P (nm)
0.0	56.5
0.3	33.2
0.4	21.2
0.5	14.9
0.6	11.1
0.7	8.6
1.0	7.0

The persistence lengths, P , calculated from a modification of Eq. 1 for fractional neutralization of negatively charged phosphates, x . The value for fully ionized DNA, $x = 0$, is taken from Table 1 for DNA on uncoated mica.

the origins of replication in *Xenopus* early embryos (34), and the switch constituted by spermidine and the restriction enzyme *Nae* I (35). It clearly affects the stability of nucleosomes in chromatin (2). The fact that natural polyamine levels rise before cell division (16,17) suggests that increased flexibility of DNA induced by charge neutralization might be important to stabilize nucleosomes and package chromatin appropriately for mitosis.

We are grateful to David Keller for discussion, Chiara Zurla, Giuseppe Lia, Laura Imperadori, and Walter Colnaghi for help with some experiments, and Paola Scaffidi and Marco Bianchi for providing the pBend2 plasmid.

This work was supported by the Italian Ministry of Instruction, Universities and Research (P.M., D.D., and L.F.), and the Human Frontier Science Program (L.F.).

REFERENCES

- Luger, K. 2003. Structure and dynamic behavior of nucleosomes. *Curr. Opin. Genet. Dev.* 13:127–135.
- Virstedt, J., T. Berge, R. M. Henderson, M. J. Waring, and A. A. Travers. 2004. The influence of DNA stiffness upon nucleosome formation. *J. Struct. Biol.* 148:66–85.
- Strauss, J. K., C. Roberts, M. G. Nelson, C. Switzer, and L. J. Maher 3rd. 1996. DNA bending by hexamethylene-tethered ammonium ions. *Proc. Natl. Acad. Sci. USA.* 93:9515–9520.
- Kosikov, K. M., A. A. Gorin, X. J. Lu, W. K. Olson, and G. S. Manning. 2002. Bending of DNA by asymmetric charge neutralization: all-atom energy simulations. *J. Am. Chem. Soc.* 124:4838–4847.
- Manning, G. S. 1989. Self-attraction and natural curvature in null DNA. *J. Biomol. Struct. Dyn.* 7:41–61.
- Manning, G. S. 1978. The molecular theory of polyelectrolyte solutions with applications to the electrostatic properties of polynucleotides. *Q. Rev. Biophys.* 11:179–246.
- Frontali, C., E. Dore, A. Ferrauto, E. Gratton, A. Bettini, M. R. Pozzan, and E. Valdevit. 1979. An absolute method for the determination of the persistence length of native DNA from electron micrographs. *Biopolymers.* 18:1353–1373.
- Bussiek, M., N. Mucke, and J. Langowski. 2003. Polylysine-coated mica can be used to observe systematic changes in the supercoiled DNA conformation by scanning force microscopy in solution. *Nucleic Acids Res.* 31:e137.
- Cherny, D. I., and T. M. Jovin. 2001. Electron and scanning force microscopy studies of alterations in supercoiled DNA tertiary structure. *J. Mol. Biol.* 313:295–307.
- van Noort, J., S. Verbrugge, N. Goosen, C. Dekker, and R. T. Dame. 2004. Dual architectural roles of HU: formation of flexible hinges and rigid filaments. *Proc. Natl. Acad. Sci. USA.* 101:6969–6974.
- Lysetska, M., A. Knoll, D. Boehringer, T. Hey, G. Krauss, and G. Krausch. 2002. UV light-damaged DNA and its interaction with human replication protein A: an atomic force microscopy study. *Nucleic Acids Res.* 30:2686–2691.
- Lu, Y., B. D. Weers, and N. C. Stellwagen. 2003. Analysis of the intrinsic bend in the M13 origin of replication by atomic force microscopy. *Biophys. J.* 85:409–415.
- Rivetti, C., M. Guthold, and C. Bustamante. 1996. Scanning force microscopy of DNA deposited onto mica: equilibration versus kinetic trapping studied by statistical polymer chain analysis. *J. Mol. Biol.* 264:919–932.
- Evilevitch, A., L. Lavelle, C. M. Knobler, E. Raspaud, and W. M. Gelbart. 2003. Osmotic pressure inhibition of DNA ejection from phage. *Proc. Natl. Acad. Sci. USA.* 100:9292–9295.
- Baumann, C. G., S. B. Smith, V. A. Bloomfield, and C. Bustamante. 1997. Ionic effects on the elasticity of single DNA molecules. *Proc. Natl. Acad. Sci. USA.* 94:6185–6190.
- Oredsson, S. M. 2003. Polyamine dependence of normal cell-cycle progression. *Biochem. Soc. Trans.* 31:366–370.
- Wallace, H. M., A. V. Fraser, and A. Hughes. 2003. A perspective of polyamine metabolism. *Biochem. J.* 376:1–14.
- Bloomfield, V. A. 1997. DNA condensation by multivalent cations. *Biopolymers.* 44:269–282.
- Sergeyev, V. G., O. A. Pyshkina, A. V. Lezov, A. B. Mel'nikov, E. I. Ryumtsev, A. B. Zevin, and V. A. Kabanov. 1999. DNA complexed with oppositely charged amphiphile in low-polar organic solvents. *Langmuir.* 15:4434–4440.
- Gosule, L. C., and J. A. Schellman. 1978. DNA condensation with polyamines I. Spectroscopic studies. *J. Mol. Biol.* 121:311–326.
- Chattoraj, D. K., L. C. Gosule, and A. Schellman. 1978. DNA condensation with polyamines. II. Electron microscopic studies. *J. Mol. Biol.* 121:327–337.
- Podesta, A., L. Imperadori, W. Colnaghi, L. Finzi, P. Milani, and D. Dunlap. 2004. Atomic force microscopy study of DNA deposited on poly L-ornithine-coated mica. *J. Microsc.* 215:236–240.
- Gossl, I., L. Shu, A. D. Schluter, and J. P. Rabe. 2002. Molecular structure of single DNA complexes with positively charged dendronized polymers. *J. Am. Chem. Soc.* 124:6860–6865.
- Deng, H., V. A. Bloomfield, J. M. Benevides, and G. J. Thomas, Jr. 2000. Structural basis of polyamine-DNA recognition: spermidine and spermine interactions with genomic B-DNAs of different GC content probed by Raman spectroscopy. *Nucleic Acids Res.* 28:3379–3385.
- Mirzabekov, A. D., and A. Rich. 1979. Asymmetric lateral distribution of unshielded phosphate groups in nucleosomal DNA and its role in DNA bending. *Proc. Natl. Acad. Sci. USA.* 76:1118–1121.
- Manning, G. S., K. K. Ebralidse, A. D. Mirzabekov, and A. Rich. 1989. An estimate of the extent of folding of nucleosomal DNA by laterally asymmetric neutralization of phosphate groups. *J. Biomol. Struct. Dyn.* 6:877–889.
- Strauss, J. K., and L. J. Maher 3rd. 1994. DNA bending by asymmetric phosphate neutralization. *Science.* 266:1829–1834.
- Sanghani, S. R., K. Zakrzewska, and R. Lavery. 1996. Biological Structure and Dynamics 1996. *Proc. Ninth Conversation.* 2:267–278.
- Williams, L. D., and L. J. Maher 3rd. 2000. Electrostatic mechanisms of DNA deformation. *Annu. Rev. Biophys. Biomol. Struct.* 29:497–521.
- Gurie, R., T. H. Duong, and K. Zakrzewska. 1999. The role of DNA-protein salt bridges in molecular recognition: a model study. *Biopolymers.* 49:313–327.
- Gurie, R., and K. Zakrzewska. 1998. DNA curvature and phosphate neutralization: an important aspect of specific protein binding. *J. Biomol. Struct. Dyn.* 16:605–618.
- Seeman, N. C. 2003. DNA in a material world. *Nature.* 421:427–431.
- Li, J., M. Gershow, D. Stein, E. Brandin, and J. A. Golovchenko. 2003. DNA molecules and configurations in a solid-state nanopore microscope. *Nat. Mater.* 2:611–615.
- Jun, S., J. Herrick, A. Bensimon, and J. Bechhoefer. 2004. Persistence length of chromatin determines origin spacing in *Xenopus* early-embryo DNA replication: quantitative comparisons between theory and experiment. *Cell Cycle.* 3:223–229.
- Conrad, M., and M. D. Topal. 1989. DNA and spermidine provide a switch mechanism to regulate the activity of restriction enzyme *Nae* I. *Proc. Natl. Acad. Sci. USA.* 86:9707–9711.